Pergamon

Tetrahedron Vol. 50, No. 21, pp. 6417-6432, 1994

0040-4020/94 $7.00+0.00

0040-4020(94)E0267-W

Conformational studies on ß-Galactopyranosyl-(1->3) and (1->4)-Xylopyranosides by NMR, Molecular Mechanics, Molecular Dynamics, and Semiempirical Calculations.

Juan Luis Asensio, Rosa López, Alfonso Fernández-Mayoralas, and Jesús Jiménez-Barbero*

Grupo de Carbohidratos, Departamento de Química Orgánica Biológica, Instituto de Química Orgánica, (C.S.I.C)., Juan de la Cierva 3, 28006 Madrid (Spain)

Abstract: The conformation of methyl 4-*O*-(ß-D-galactopyranosyl)-ß-D-xylopyranoside (**1**) and benzyl 3-*O*-(ß-D-galactopyranosyl)-ß-D-xylopyranoside (**2**) has been studied by NMR spectroscopy, assisted by molecular mechanics, molecular dynamics, and semiempirical methods. Both compounds show moderate flexibility and the shape of the global minimum of both molecules is very similar, although the xylose ring shows an important displacement when going from **1** to **2**.

ß-D-Galactopyranosyl-D-xyloses are fragments of proteoglycans[1] and xyloglucans[2] which play a number of biological roles. In recent years, the disaccharide Gal-ß-(1->4)-Xyl, which resembles lactose (Gal-ß-(1->4)-Glc) has been used to modify biosynthetic pathways in which lactose is involved[3], and has been proposed as a non-invasive tool to evaluate *in vivo* the activity of intestinal lactase in animals[4]. We have previously reported on the synthesis of methyl 4-*O*-(ß-D-galactopyranosyl)-ß-D-xylopyranoside (**1**) and benzyl 3-*O*-(ß-D-galactopyranosyl)-ß-D-xylopyranoside (**2**) by enzymatic galactosidation of the corresponding xylose derivatives[5]. In addition, based on our results on the galactosidation of different xylopyranosides, we have postulated[6] that different complexes between the xylopyranoside and the enzyme are formed when ß-(1->4) or ß-(1->3)-linked disaccharides are produced. Our hypothesis involved a different orientation of the xylopyranoid ring (*ca.* 180 flip) in the two different complexes. Assuming that the enzymatic reaction takes place under kinetic control, the orientation of the xylose ring in the transition state could be related to the major conformation of the synthetic products, in this case, disaccharides **1** and **2**. We now report on the conformational study of **1** and **2** using NMR spectroscopy, assisted by Molecular Mechanics (MM), Molecular Dynamics (MD), and semiempirical calculations, in order to evaluate the extension of flexibility of these molecules, and to assess the degree of agreement between the different force fields employed in the theoretical calculations, and the experimental NOE results.

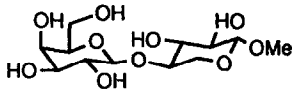

1

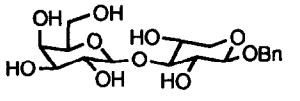

2

RESULTS AND DISCUSSION

Table 1. Interatomic Distances, Energy Differences, and Populations for the Low Energy Conformers of **1**.

	Conformer(Φ/Ψ)				
	A 51/-1	**D** 27/175	**E** 170/4	**C** -23/-28	**B** 24/-55
	ΔE (Kcal/mol)				
AMBER (SINGLE POINT)					
ε=78	0.0	1.3	0.5	A	A
POP(%)	63.4	7.7	28.9	A	A
ε=4*r	1.0	0.0	1.7	A	A
POP(%)	15.0	80.3	4.7	A	A
ε=1*r	1.4	0.0	2.4	A	A
POP(%)	8.6	89.8	1.6	A	A
ENSEMBLE AVERAGE(ε=78)					
POP(%)	72.0	8.0	20.0	A	A
MM2 (SINGLE POINT)					
ε=78	0.0	3.8	4.8	2.5	1.9
POP(%)	94.5	0.2	0.0	1.4	3.9
ε=1	0.2	2.3	3.5	0.8	0.0
POP(%)	35.4	1.1	0.1	13.1	50.3
CVFF (SINGLE POINT)					
ε=1	0.0	1.6	4.1	A	A
POP(%)	93.5	6.4	0.1	A	A
ENSEMBLE AVERAGE					
POP(%)	91.1	8.1	0.8	A	A
AM1 (SINGLE POINT)					
vacuo	0.32	0.58	0.00	A	A
POP(%)	29.8	19.3	50.9	A	A
AM1 (SINGLE POINT)					
solution	0.87	0.06	0.00	A	A
POP(%)	10.9	42.3	46.8	A	A
	Distance(Å)				
$r_{1'4}$	2.39	>3.5	>3.5	2.31	2.42
$r_{1'3}$	>3.5	1.8	>3.5	3.55	3.44
$r_{1'5eq}$	3.14	>3.5	>3.5	>4	>4
$r_{2'4}$	>3.5	>3.5	1.94	>3.5	>3.5

A.-Converges to Conformer A.

Tables 1 and 2 show the values of the steric energies, of the estimated populations, and of the relevant interproton distances of the different conformers of **1** and **2**, obtained, as described in experimental, by using the AMBER[7] and CVFF[8] force fields, in comparison to those previously reported for **1** by using the MM2 program. Due to the presence of a number of electronegative atoms, these energies should be taken as approximate since they are variable at least 0.5 Kcal/mol. The single-point populations are calculated from the energy values for the corresponding local minima, and not for the conformers having the exact Φ/Ψ value. The torsion angle values for the different minima did not differ more than 10º from the figures of Tables 1-2, independently of the force field or the dielectric constant used.

Table 2. Interatomic Distances, Energy Differences, and Populations for the Low Energy Conformers of **2**.

Distance(Å)	Conformer(Φ/Ψ)				
	A	**D**	**E**	**B**	**C**
	48/7	23/171	166/8	-23/-22	20/-35
			ΔE (Kcal/mol)		
AMBER (SINGLE POINT)					
ε=78	0.0	1.4	0.4	A	A
POP(%)	65.3	5.5	29.2	A	A
ε=4*r	1.7	0.0	1.0	A	A
POP(%)	5.2	79.5	15.3	A	A
ε=1*r	2.4	0.0	1.4	2.4	A
POP(%)	1.6	88.4	8.4	1.6	A
ENSEMBLE AVERAGE (ε=78)					
POP(%)	74.0	8.0	18.0	A	A
CVFF (SINGLE POINT)					
ε=1	0.0	2.5	1.9	A	A
POP(%)	94.6	1.4	4.0	A	A
ENSEMBLE AVERAGE					
POP(%)	98.5	0.5	1.0	A	A
AM1 (SINGLE POINT)					
vacuo	1.57	1.03	0.00	A	A
POP(%)	5.8	14.2	80.0	A	A
AM1 (SINGLE POINT)					
solution	0.00	0.31	5.14	A	A
POP(%)	62.7	37.3	0.0	A	A
			Distance(Å)		
$r_{1'4}$	>4.0	1.9	3.8	>4.0	4.0
$r_{1'3}$	2.4	>3.5	>3.5	2.2	2.2
$r_{1'2}$	3.9	2.8	>4.0	>4.0	>4.0
$r_{2'3}$	>3.5	>3.5	2.1	>3.5	>3.5

A.-Converges to Conformer A

Relaxed energy plots of the isoenergy contours obtained by using the AMBER and CVFF force fields for compounds **1** and **2** are given in Figures 1 and 2, respectively. Although the CVFF is a general MM programme not specifically parametrized for carbohydrates, and therefore does not include any extra potential to account for the *endo-* or *exo*-anomeric effects[9], its use in the conformational study of different oligosaccharides has produced satisfactory results[10]. On the other hand, the AMBER force field has been recently parametrised to deal with carbohydrate molecules[11]. After energy minimization, it can be observed that, in all cases, there is a broad low energy region, which depending on the orientation of the hydroxyl groups can be described by different conformers with rather small energy barriers among them, and two separated smaller islands.

Figure 3 shows views of these low energy conformers for **1** and **2**. The previously reported X-ray structures for different ß(1->4) and ß(1->3) equatorial linked disaccharides[12,13] are included in the low energy regions for **1** and **2**.

Although, generally speaking, all the force fields used in this work provide remarkably similar geometries for the local minima, the associated energies are rather different. In addition, some of the local mimima detected by the MM2 program are not stable when using AMBER and CVFF and converge to minimum A. Plots of the levels of population of the different regions, calculated from the CVFF or AMBER energies are also shown in Figures 1 and 2. Both adiabatic maps show a very similar shape, although the surface of **1** seems to be more extended along Ψ axes, particularly when considering the AMBER results.

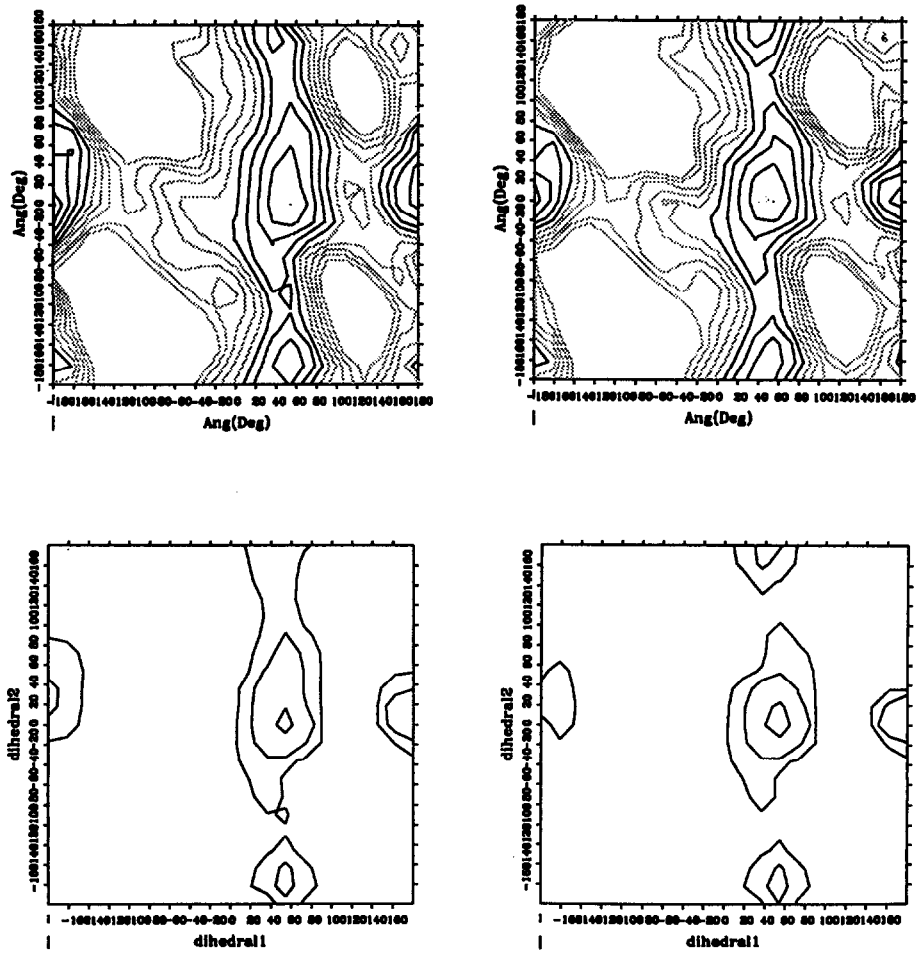

Fig. 1. Adiabatic maps (above) of the isoenergy contours (1 Kcal/mol) and populations (below) calculated from the relaxed steric energy plots obtained by using AMBER for **1** (left) and **2**.(right). The level contours of populations are given at 10%, 1%, and 0.1%. Φ is indicated horizontally, and Ψ along the vertical axis.

This fact is reasonable, in principle, since the site of attachment of the glycosidic linkage to the xylose moiety shows either two equatorial oxygen substituents (compound **2**) or only one equatorial oxygen and two hydrogens (**1**). Therefore, according to the observations reported[14] by Anderson *et al.*, it is to be expected a higher rigidity along Ψ angle for **2**. Depending on the method of calculation, the population of the different regions is rather distinct. Thus, according to the previous MM2 results[12], the low energy region of **1**, described by Φ=50±40º, Ψ=-20±40º, appears to be populated in more than 90% extent, while the two minor islands described by conformers D and E are populated less than 5% at 40º. However, although the calculation of the conformer populations making use of relaxed AMBER maps (ε=78 D) also locates the A region as the more heavily populated, predicts that its population is of only 72%. Islands E and D, on the other hand, are populated in 20 and 8% extent, respectively. The calculation from the the single-point energy conformers predicts a smaller population of the central region, only 63%, while that of E increases to 29%.

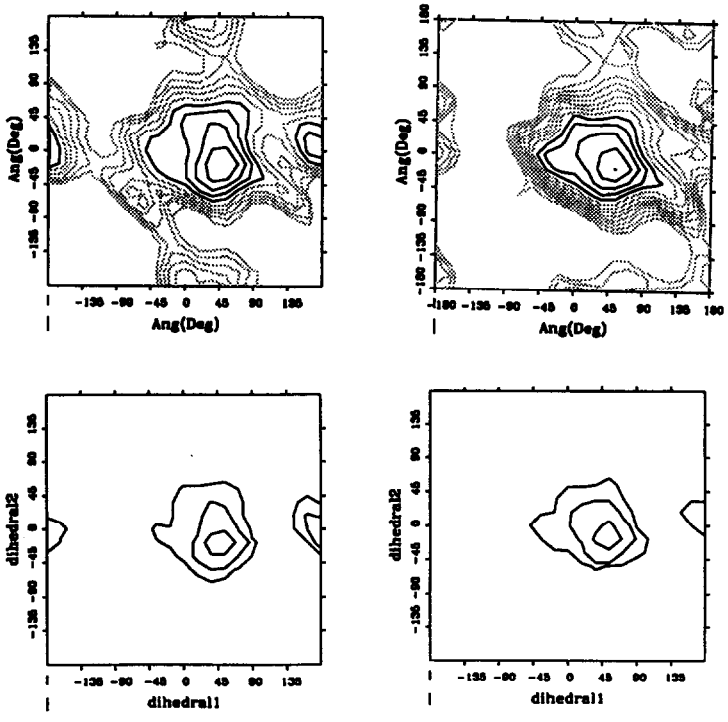

Fig. 2.-Adiabatic maps (above) of the isoenergy contours (1 Kcal/mol) and populations (below) calculated from the relaxed steric energy plots obtained by using CVFF for **1** (left) and **2**.(right). The level contours of populations are given at 10%, 1%, and 0.1%. Φ is indicated horizontally, and Ψ along the vertical axis.

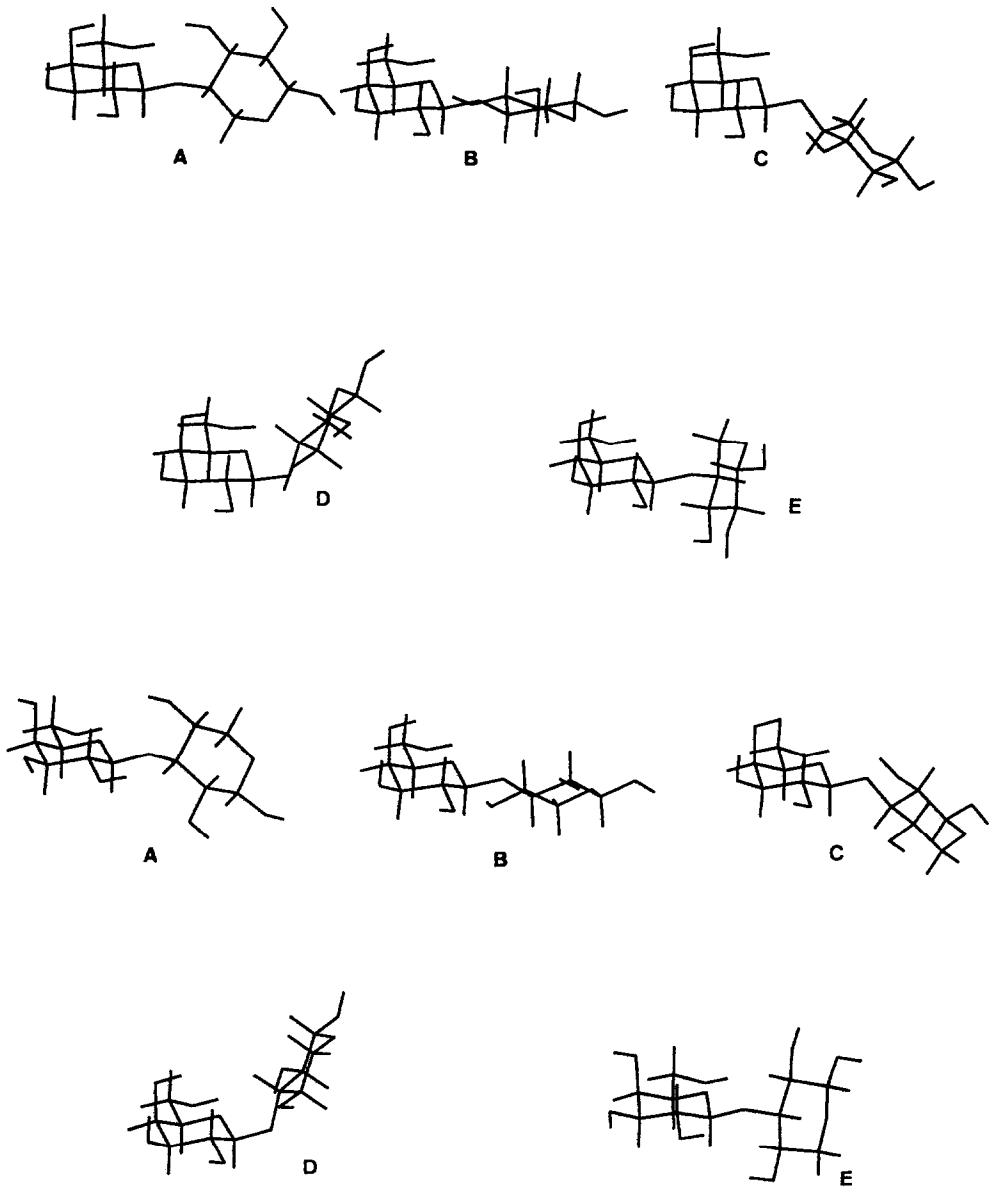

Fig. 3. Views of the low energy conformers of **1** (above) and **2** (below). In both cases, approximate Φ/Ψ angles are as follows: A (48/7), B (20/-35), C (-23/-22), D (166/8), E (23/171).

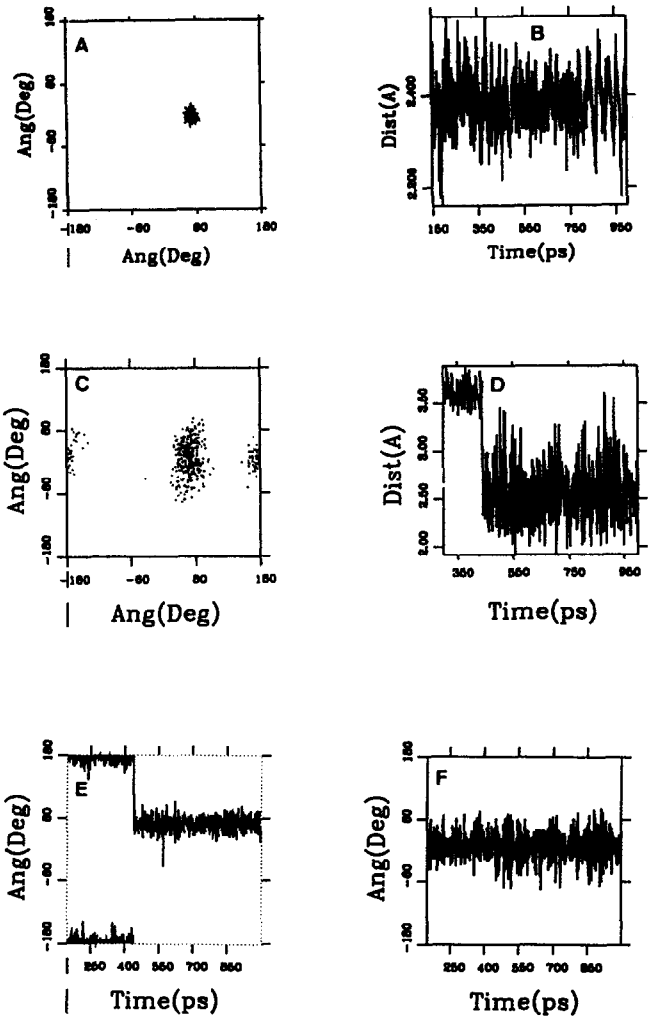

Fig. 4. Trajectory plots of two MD simulations for **1**. Top, (CVFF, ε=1 D, time 1 ns), starting from conformer A. From left to right: (A) Trajectory of the simulation in Φ/Ψ space. (B) History of H-1'-H-4. Bottom, (AMBER, ε=80, 1 ns), starting from conformer D. (C) Trajectory of the simulation in Φ/Ψ space. (D) History of H-1'-H-4. (E) History of Φ angle. (F) History of Ψ.

The use of the CVFF force field, on the other hand, accounts for a higher population of the region defined by minimum A, which amounts to 90%. The population of islands D and E is only marginal (<5%). The use of quantum mechanical methods is not widely spread in oligosaccharide conformational problems, mainly due to the time-consuming calculations involved[15]. The optimization of the geometries of three local minima of the adiabatic map by the AM1 method[16] provides, in this case, very slight energy differences, which indicates that the three different regions are present in solution. Thus, the semiempirical calculations indicate a 30:19:51 distribution *in vacuo*, and, after estimation of the solvation energy by the AMSOL[17] program,a 11:42:47 equilibrium in water among the major conformers representing regions A:D:E, respectively. It is noteworthy to mention that the possibility of the existence of islands D and E in solution cannot be discarded since their existance has been reported for some ß-(1->4)-linked oligosaccharides[18]. For compound **2**, from the energies of the relaxed AMBER surfaces, the corresponding low energy region of **2** described by Φ=50±40º, Ψ=20±35º appears to be populated in more than 74% extent, while the two minor conformers D and E are populated in 8 and 18% extent at 40°. The use of single point conformers provides again a higher population for E, which increases to 29%, while A region decrease to 65%. As stated above, the central region (A conformer) is much more stable, according to the CVFF calculations, and its population is 93%, while that of D and E is again less than 5%. The use of single point conformers only partially modify these figures. Finally, the AM1 method predicts 6:14:80 and 63:37:0 equilibria *in vacuo* and in solution, respectively. It has to be noted that all these populations are calculated from energy values which correspond to enthalpies and not to true free energies. Although the calculations are only approximated, an estimation of the vibrational free energies[19] using CVFF for the low energy conformers of **1** and **2** indicates that, in both cases, the central region should be more populated, since their associated entropies are significantly higher for conformers of type A (between 0.5-0.9 Kcal/mol at 40º). The normal mode vibrational analysis, according to the AM1 Hamiltonian does not concludes the same results, since the calculated entropy for A is in between that for D and E, respectively. Anyway, it has to be mention that this method only provide qualitative estimations for molecules with internal rotations. As a further step, the conformational stability of the minima was studied by using molecular dynamics simulations (MD) with CVFF and AMBER . Different conformations of **1** and **2** were used as input geometries for independent 0.5-2 ns simulations at 300 or 400°K. Several trajectories are displayed in Figures 4 and 5. In all cases, no chair to chair or chair to boat interconversions were observed. For both ß(1->4) and ß(1->3) linkages, the average Φ and Ψ angles were calculated to be 50±15º and 0±20º, depending on the starting conformer. It can be observed that the trajectories remained most of the time in the low energy region close to form A. In fact, only when the calculation started from geometry E, the trajectory spent a fraction of time within this island (*ca.* 300 ps), although the trajectory went again to the low energy region. Also, when the starting geometry was that of D, the simulation resulted in a transition to region A within a few ps. Therefore, according to the MD simulations, minimum energy conformers D and E are not stable enough in comparison to A, when external factors such as stabilization by external hydrogen or covalent bonds or non polar contacts are not involved. In some cases, for the 400ºK simulations, several transitions between the possible orientations of the galactoses lateral chains were observed.(Fig 6).

NMR spectroscopy can be used to distinguish the presence of either conformer[20]. All the low energy region described by conformers A-C of compound **1** has short distances between H-4 and H-1', H-3 is close to H-1' in conformer E, H-4 close to H-2' in conformer D, and there is an unique contact between H-1' and H-5_{eq} for conformer A, respectively. In addition, HO-3 and O-5' of A and B can be intramolecularly hydrogen bonded since both oxygen atoms are less than 3.0 Å apart. These structural characteristics are shown in Tables I and II.

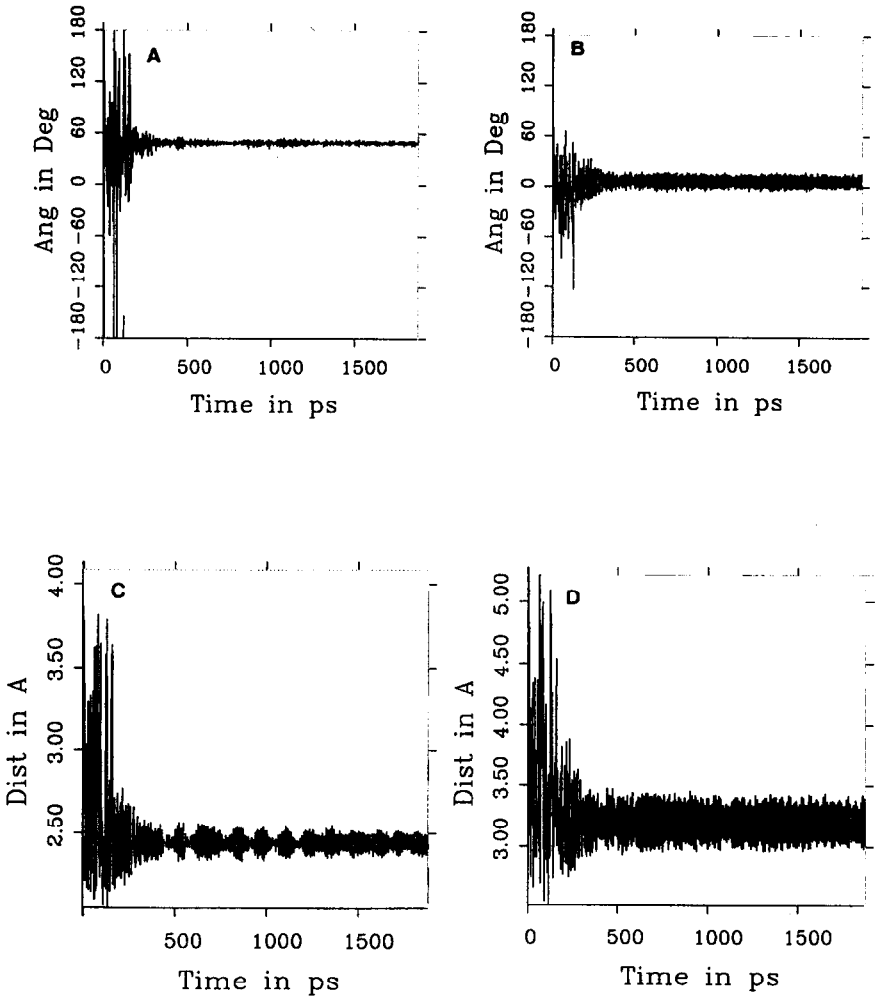

Fig. 5. Trajectory plots of one MD simulation (CVFF, ε=1 D, time 2 ns) for **2**, starting from A region. From left to right and top to bottom: (A) History of Φ angle, (B) History of Ψ. (C) History of H-1'-H-3. (D) History of H-1'-H-4.

Table 3. ^{1}H-NMR Chemical Shifts (δ, ppm) for **1**-**2** in D_2O Solution at 40 °C.

Proton	Compound			
	1	**2**	**1**	**2**
	Xylose residue		Galactose residue	
H-1	4.53	4.54	4.48	4.65
H-2	3.37	3.52	3.52	3.60
H-3	3.59	3.68	3.66	3.67
H-4	3.86	3.75	3.93	3.93
H-5*ax*	3.41	3.36	3.71	3.70
H-5*eq*	4.12	4.03		
H-6'S			3.75	3.76
H-6'R			3.82	3.80

Hydroxymethyl conformation. Gal $H6_{proR}$ and $H6_{proS}$ were assigned as previously reported for similar derivatives[21]. The distribution of rotamers was calculated, following well established methodology, assuming a *gt:tg:gg* equilibrium[22]. The observed couplings agree with combinations of the *gt* and *tg* rotamers, being the *gt* family populated in extensions >65%. These experimental results are in fair agreement with those calculated from the AMBER energy surfaces, which predict *gt* populations of 61 and 62% for **1** and **2**, respectively.

Analysis of NOE data- The conformational analysis of oligosaccharide structures based on NOE data can be performed in several ways[23]. Qualitatively, the existence of NOE between H-1' and H-4 and not between H-2' and H-4 implies that compound **1** spends most of its time in the region defined by local minima A-C. Besides, the presence of NOE between H-1' and H-5_{eq} protons indicate that the region defined by minimum A is populated to some extent. On the other hand, the small but detectable H-1'-H-3 NOE indicates that the region defined by conformer A is not the only one populated in water solution, and that conformers B, C, and/or E are also present. The corresponding average distances for H-1'-H-4, H-1'-H-3, H2'-H-4, and H-1'-H5_{eq} proton pairs from MD simulations are 2.30 Å, 3.20, 3.40 Å, and 2.60 Å, respectively, although oscillations could be observed. On the other hand, the calculation from the adiabatic AMBER map provides values of 2.7, 3.8, 3.2, and 2.9 Å, ($\langle r^{-3} \rangle$ averaging) or 2.6, 3.2, 2.7 and 2.7 Å ($\langle r^{-6} \rangle$ averaging), respectively. According to these values, besides those observed NOEs, we should also expect the presence of NOE between H-2' and H-4 protons. In principle, a more rigorous method to evaluate the experimental data is to use the geometries of the different minima to calculate the expected NOE[24] *via* a complete relaxation matrix[25] approach using either one conformation or an average[26] according to a Boltzmann distribution function[27] at a given temperature. The results following this methodology by using the protocole described in the experimental part are collected in Table 4. The correlation time was estimated from the fitting between the calculated and experimental intensities of H-1'-H-3' and H-1'-H-5'. The comparison among the observed and calculated interresidue cross peaks H-1'-H-4, H-1'-H-3, and H-1'-H-5_{eq} for the different individual minima showed that a satisfactory match could be obtained by considering the presence of certain flexibility (Φ=60±20º and Ψ=10±20º) around form A in the conformational equilibrium, along with a small participation (*ca.* 5-10%) of conformer E. A more precise quantitation of the population of both states is precluded by the uncertainty in the time scale of motion around the linkages.It is important to mention that the calculation of the NOEs from the AMBER energies (ε=78) provided H-1'-H-4 intensities noticeably smaller than those measured along with larger NOE values for the H-1'-H-3 (E region) and observable H-2'-H-4 (D region) intensities.

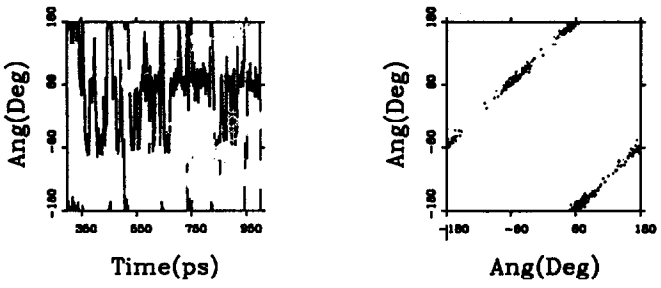

Fig. 6.- Transitions between the possible orientations of the galactose lateral chain of **1** (400°K, AMBER). History of ω (H-5-C-5-C-6-O-6) torsion angle (left). Trajectory of the simulation in torsional space (right): ω angle is indicated horizontally and O-5-C-5-C-6-O-6 torsion angle along the vertical axis. Conformations *gt* and *tg* are strongly predominant along the whole MD simulation.

The superimposition of these relevant interproton distances with the corresponding conformational maps are given in Figure 7. The observation of one or two interresidue NOEs can impose constraints in the potential energy map to verify the existence of a given conformation[20]. The previous step for the analysis of the NOE data was the assignment of the different resonances through a combination of regular COSY and HMQC techniques. The chemical shifts for **1** and **2** are shown in Table 3. The observed couplings (data not shown) agree with $^4\underline{C}_1$ chair conformations for all the pyranoid rings of **1** and **2**.

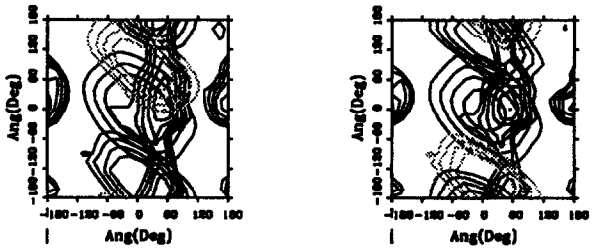

Fig. 7.-Superimposition of the relevant interproton distances with the energy maps of **1** (left) and **2** (right). Distance levels are drawn at 2.3, 2.6, 2.9, and 3.2 Å. For **1**, H-1'-H-4 (centre), H-1'-H-5eq (above), and H-1'-H-3 (below) distances are indicated. For **2**, H-1'-H-3 (centre), H-1'-H-2 (above), and H-1'-H-4 (below).

Table 4. Experimental and Calculated Steady State NOEs (H-1', Sat.time=10 s) for **1** at 37ºC in D_2O Solution, at 300 and 500 MHz.

Proton pair	Intensity (%)						
	a	b	c	d	e	f	g
H-1'/2'	7	6	6	6	6	5	6
H-1'/3'	10	9	10	10	10	9	10
H-1'/4'	-3	-2	-2	-2	-2	-2.5	-2.5
H-1'/5'	12	11	11	11	11	13	12
H-1'/4	15	13	13	-	12	8	13
H-1'/5eq	3	2	2		2	3	2.5
H-1'/3	3	2	--	32	3	3	0.5
H-2'/4	--	--	--	--	--	0.8	0.6

[a] Experimental 300 MHz. [b] Exp. 500 MHz. [c] Theoretical from minimum A. [d] Theor. from minimum E. [e] 95:5 A:E equilibrium. [f] Ensemble average Amber. [g] Ensemble average CVFF. In all cases $\tau_c=0.06*10^{-9}$ s

However, according to the experimental data, the presence of conformers D or E in an appreciable extent (>5%) can be discarded. The use of AMBER with smaller dielectric constants produce even worse results, since D population became higher (Table 1). On the other hand, although not especially parametrized for carbohydrates, the CVFF energies are more consistent with the experimental NOEs. Therefore, according to our results, the AMBER force field, when used in these conditions (bulk dielectric constant), does not correctly reproduce[28] the conformational properties of **1** (and **2**, see below). Although the application of the AM1 Hamiltonian has been performed in a less systematic way, a similar behavior is observed with these calculations and the fit to the experimental NOE data is poor. Interestingly, the AM1 charges are much closer to those employed by the CVFF program than to those used by AMBER.

The presence of NOE between H-1' and H-3 and not between H-1' and H-4 indicates that the conformation of **2** can be defined by the central region. However, the presence of NOE between H-1' and H-2 indicates that minimum A alone can not explain the experimental data. The corresponding average distances for H-1'-H-3, and H-1'-H-2 from MD simulations are 2.40 Å and 2.95 Å, respectively, although oscillations were also observable. The results following the relaxation matrix methodology are collected in Table 5.

Table 5. Experimental and Calculated ($\tau_c=0.06*10^{-9}$ s) Steady State NOEs (H-1', Saturation Time=10 s) for **2** at 37ºC in D_2O Solution, at 300 and 500 MHz.

Proton pair	Intensity (%)				
	a	b	c	d	e
H-1'/2'	8	7	6	6	6
H-1'/3'	10	9	9	9	9
H-1'/4'	-3	-2	-2	-2.5	-2.5
H-1'/5'	11	10	10	13	12
H-1'/4	--	--	--	3	--
H-1'/3	17	14	15	10	13
H-1'/2	2	2	1	2	1
H-2'/3	--	--	--	--	--

[a] Experimental 300 MHz. [b] Exp. 500 MHz. [c] Theoretical from minimum A. [d] Ensemble average Amber [e] Ensemble average CVFF

The comparison among the observed and calculated interresidue cross peaks H-1'-H-3, and H-1'-H-2 for the different individual minima showed that a satisfactory match could be obtained by considering the presence of flexibility around minimum A (Φ=60±20° and Ψ=10±20°). The presence of other conformers in an appreciable extent (>5%) can be discarded since they would produce H-1'-H-3 intensities noticeably smaller than those measured along with much larger NOE values for the H-1'-H-4 contact, that was not detected. Again, as described for **1**, the calculation of the ensemble average NOEs from AMBER energies predicts smaller H-1'-H-3 intensities than those observed. However, the experimental NOE data can be satisfactorily explained by considering the presence of conformers located in the low energy region alone. As stated above, the CVFF results have a better agreement with the experiment than the AMBER and the AM1 methods.

These results indicate that the extent of flexibility around the ß(1-4) linkage of **1** and the ß(1->3) linkage of **2** in water solution is rather limited, and that less than 5% of the complete potential energy surfaces are populated in solution. Therefore, for both linkages, the recognition of conformers of other regions should be accompanied by the formation of several hydrogen bonds or stabilizing van der Waals contacts to override the important energy barrier between the low energy area and the different islands.

According to our results, the glycosidic bonds of **1** and **2** are neither as flexible as observed for the Gal-ß(1->4)-Glc linkage within the GM1 ganglioside in dimethyl sulfoxide[29], nor as rigid as deduced for the same moiety in the GM3 analogue[30], the Le^X trisaccharide[31], 6'-*O*-sialyllactose[32], and the Gal-ß(1->4)-Xyl linkage in two proteoglycan fragments[33]. Compound **1** shows a moderate flexibility, similar to that proposed for ß-(1->4)-linked lactosides[10,12,34] and xylobiosides[35]. The MD simulations produced average O-5´-O-3 distances of 2.95±0.10 Å indicating the possible presence of intramolecular hydrogen bond. With regard to **2**, it seems to be also fairly rigid, with reduced oscillations around a global shape similar to that reported for the Gal-ß(1->3)-Glc moiety of the Le^a group[36]. The existence of intramolecular O-5'-O-4 hydrogen bond is also possible, according to the calculated average distance. A superimposition of the global minima for both compounds is shown in Figure 8. The global shape of both molecules is very similar, although the xylose ring shows an important displacement when going from **1** to **2**. Although other explanations could also be possible, the calculated major conformers satisfactorily explain the results observed in the enzymatic galactosidation of xylopyranosides[5,6].

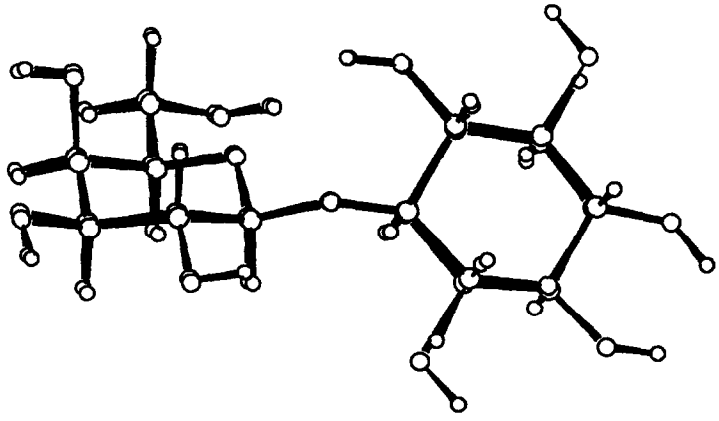

Fig. 8.-Superimposition of the global minima for compounds **1** and **2**.

EXPERIMENTAL

Materials.- The syntheses of compounds **1** and **2** have been reported elsewhere[5,6].

NMR experiments.- NMR spectra were recorded at 40 °C in D_2O, on Varian XL-300 and Unity 500 spectrometers. Proton chemical shifts were referenced to residual HDO at δ 4.61 ppm. The steady state NOE experiments were performed through the interleaved differential technique using a saturation delay of 10 s.

Conformational calculations.- Glycosidic torsion angles are defined as Φ H-1'-C-1'-O-1'-C-4, and Ψ C-1'-O-1'-C-4-H-4 for **1**, and Φ H-1'-C-1'-O-1'-C-3, and Ψ C-1'-O-1'-C-3-H-3 for **2**. Relaxed (Φ,Ψ) potential energy maps[15] were calculated for compounds **1** (as methyl glycoside) and **2** by using the AMBER[7] and CVFF[8] force fields. Only the *tg* and *gt* conformations of the lateral chain were used for the galactose residue[21,22], since they have been shown to be rather more stable than the alternative *gg* conformer. The starting position for the secondary hydroxyl groups was set as *rr* (anti-clockwise) or *cc* (clockwise). Therefore, four different energy maps were built for each disaccaride and each force field. In total 6400 conformers were calculated. The previous step involved the generation of the corresponding rigid residue maps by using a grid step of 18º. Then, every Φ,Ψ point of this map was optimised to build the relaxed one. From these data, adiabatic CVFF and AMBER surfaces were built for both **1** and **2**. In order to explore the possibility of additional local minima not detected by this protocol, the MM2-low energy conformers[12] found previously for the ß-methyl analogue of **1** were built and submitted to further minimization by using AMBER and CVFF. For compound **2**, different conformers based on the previously reported X-ray and molecular mechanics conformers for laminaribiose analogues (Glc-ß-(1->3)-Glc) were also built and minimized (Φ/Ψ, 54-29º/14-8º, or Φ/Ψ, 42-28º/-38 to -52º)[10]. Dielectric constants of 1 and 78 D were used for the CVFF calculations, while distance dependent dielectric constants (1, 4, and 78 D) were employed for the AMBER minimizations. The low energy conformations from the adiabatic maps were also optimized by semiempirical methods at the AM1 level[16]. The heats of formation were obtained by minimizing the total energy with respect to all geometric variables, using the BFGS procedure. The adequate choice of the convergence criteria implied the use of the PRECISE option. Their corresponding solvation energies were estimated by using the AMSOL[17] program. Different geometries describing local minima were then taken as starting structures for Molecular Dynamics calculations *in vacuo* by using AMBER and CVFF as integrated in the Discover 2.9 program[37]. The MD simulations were performed at 300ºK and 400ºK, with dielectric constants of 78, 1, and/or 4*r, and a time step of 1 fs. The equilibration time was considered to be 100-200 ps while the total simulation time was 520 ps, 1020 or 2000 ps. Trajectory frames were saved every 1 ps. The trajectories were then examined with the Analysis module of INSIGHT II[38]. The steady state 1D-NOE were calculated according to the complete relaxation matrix method by using the NOEMOL[39] program for the proton coordinates of the obtained local minima, for conformers included in regions centered in the local minima geometries, for which Φ and Ψ differed up to 40º in 10º steps, and for a Boltzmann distribution of all the conformers, calculated from the relaxed relative energies at 310 °K. Isotropic motion or motion according to a symmetric top[28,39], and external relaxation of 0 and/or 0.1s were assumed in different calculation process. Only the best results are shown in Tables 4 and 5. Since NOEs are extremely dependent on the correlation time, different τ_c values were used in order to best match between the experimental and the calculated NOE for a given intraresidue proton pair. For the obtention of the ensemble average NOEs, the relaxation rates were estimated assuming r^{-3} or r^{-6} averaging of the interproton distances, in two separate calculations.

ACKNOWLEDGMENTS

Financial support by DGICYT (PB90-0076, PB87-0367), Comunidad Madrid (C258/91), and EC (Bridge Prog., BIOT-CT90-0176) is acknowledged. R. L. and J.L.A. thank Europharma S. A. for a fellowship. We thank Prof. Martín-Lomas for his interest and support.

REFERENCES AND NOTES

1. (a) Lindahl, V.; Roden, L. in *Glycoproteins*; Elsevier; Amsterdam. 1972; pp 491-517. (b) Hardingham, T. E.; Fosang, A. J. *Faseb J.* **1992**, *6*, 861-870.
2. Albersheim, P.; Darvill, A.; Augur, C.; Cheong, J.-J., Eberhard, S.; Hahn, M. G.; Marfa, V. Mohhnen, D.; O' Neill. M. A.; Spiro, M. D.; York, W. S. *Acc. Chem. Res.* **1992**, *25*, 77-.
3. Freeze, H. H.; Sampath, D.; Varki, A. *J. Biol. Chem.* **1993**, *268*, 1618-1627.
4. (a) Rivera-Sagredo, A.; Fernández-Mayoralas, A.; Jiménez-Barbero, J.; Martín-Lomas, M.; Villanueva, D.; Aragón, J. J. *Carbohydr. Res.* **1992**, *228*, 129-136. (b) Aragón, J. J.; Fernández-Mayoralas, A. Jiménez-Barbero, J.; Martín-Lomas, M.; Rivera-Sagredo, A.; Villanueva, D. *Clin. Chim. Acta.* **1992**, *210*, 221-226.
5. López, R.; Fernández-Mayoralas, A. *Tetrahedron Lett.* **1992**, *33*, 5449-5452.
6. López, R.; Fernández-Mayoralas, A. *J. Org. Chem.* **1994**, *59*, 737-745.
7. Weiner, S. J.; Kollman, P. A.; Case, D. A.; Singh, U. C.; Ghio, C. *J. Am. Chem. Soc.* **1984**, 106, 765- 784.
8. Hagler, A. T.; Lifson, S., Dauber, P. *J. Am. Chem. Soc.* **1979**, *101*, 5122-5130.
9. Lemieux, R. U.; Chu, N. J. *Abstracts of Papers*, 133rd National Meeting of ACS, San Francisco, 1958, 31N
10. Fernández, P.; Jiménez-Barbero, J. *Carbohydr. Res.* **1993**, *248*, 15-36, and references therein.
11. Homans, S. W.; *Biochemistry* **1990**, *29*, 9110-9118.
12. Rivera-Sagredo, A.; Solís, D.; Díaz-Mauriño, T.; Jiménez-Barbero, J.; Martín-Lomas, M. *Eur. J. Biochem.* **1991**, *197*, 217-228, and references therein.
13. Noguchi, K.; Okuyama, K.; Kitamura, S.; Takeo, K. *Carbohydr. Res.* **1992**, *237*, 33-42, Dowd, M. K.; French, A. D.; Reilly, P. J.; *Carbohydr. Res.* **1992**, *223*, 15-36, and references therein.
14. Anderson, J. E.; Watson, D. G.; *J. Am. Chem. Soc.* **1992**, *114*, 1517-1518.
15. Dieter, K. M.; Stewart, J. P.; *ACS Symp. Ser.* **1990**, *430*, 31-41, and references therein.
16. Dewar, M. J. S.;, Zoebisch, E. G.; Healy, E. F.; Stewart, J. J. P. *J. Am. Chem. Soc.* **1985**, *107*, 3902-3909.
17. Cramer, C. J.; Lynch, G. L.; Truhlar, D. G. *QCPE* program 606, Chemistry Department, Indiana Universi Bloomington, IN, 1992.
18. (a) Bernabé, M.; Fernández-Mayoralas, A.; Jiménez-Barbero, J.; Martín-Lomas, M.; Rivera, A. *J. Chem. Soc. Perkin Trans. II* **1989**, 1867-1873. (b) Bourne, Y.; Rouge, P.; Cambilleau, C. *J. Biol. Chem.* **1992**, *267*, 197-203. (c)
19. Hagler, A. T.; Stern, P. S., Sharon, R.; Becker, J. M.; Naider, F.*J. Am. Chem. Soc.* **1979**, *101*, 6842-6852.
20. (a) Bock, K. *Pure Appl. Chem.* 1983, 55, 605-622. (b) Meyer, B. *Top. Curr. Chem.* **1990**, *154*, 141-208.

21. (a) Nishida, Y.; Ohrui, H.; Meguro, H. *Tetrahedron Lett.* **1984**, *25*, 1575-1578. (b) Mackie, D. M.; Maradufu, A.; Perlin, A. S. *Carbohydr. Res.* **1986**, *150*, 23-33. (c) Nishida, Y.; Hori, H.; Ohrui, H.; Meguro, H. *J. Carbohydr. Chem.* **1988**, *7*, 239-250.
22. Bock, K.; Refn, S.; *Acta Chem. Scand.* **1987**, *B41*, 469-472.
23. (a) Brisson, J. R.; Carver, J. P.; *Biochemistry*, **1983**, *22*, 1362-1368. (b) Miller, K. E.; Mukhopadhyay, C.; Cagas, P.; Bush, C. A. *Biochemistry*, **1992**, *31*, 6703-6709, and references therein.
24. Imberty, A.; Tran, V.; Perez, S. *J. Comput. Chem.* **1989**, *11*, 205-216. (b) Cagas, P.; Bush, C. A. *Biopolymers*, 1990, *30*, 1123-1138.
25. Neuhaus, D.; Williamson, M. P.; *The Nuclear Overhauser Effect in Structural and Conformational Analysis* 1989 VCH Publishers, NY.
26. Peters, T.; Brisson, J. R.; Bundle, D. R. *Can. J. Chem.* **1990**, *68*, 979-988, and references therein.
27. Cumming, D. A.; Carver, J. P. *Biochemistry.* **1987**, *26*, 6664-6676.
28 It has been recently reported that AMBER may be of low accuracy in regions far from the global minimum. Rutherford, T. J.; Partridge, J. Weller, C. T.; Homans, S. W. *Biochemistry.* **1993**, *32*, 12715-12724.
29. Poppe, L.; von der Lieth, C. W.; Dabrowski, J. *J. Am. Chem. Soc.* **1990**, *112*, 7762-7771.
30. Siebert, H. C.; Reuter, G.; Schauer, R.; von der Lieth, C. W.; Dabrowski, *Biochemistry*, **1992**, *31*, 6962-6971.
31. Mukhopadhyay, C.; Miller, K. E.; Bush, C. A. *Biopolymers*, **1994**, *31*, 21-29, and references therein.
32. Poppe, L.; Stuike-Prill, R. Meyer, B.; van Halbeek, H.; *J. Biomol. NMR.* **1992**, *2*, 109-136.
33. (a) Choe, B.-Y., Ekborg, G. C.; Roden, L.; Harvey, S. C., Krishna, N. R. *J. Am. Chem. Soc.* **1991**, *113*, 3743-3749. (b) Krishna, N. R.; Choe, B.-Y., Prabhakaran, M. Ekborg, G. C.; Roden, L.; Harvey, S. C. *J. Biol. Chem.* 1990, 265, 18256-18261.
34. Rivera-Sagredo, A.; Jiménez-Barbero, J.; Martín-Lomas, M. *Carbohydr. Res.* **1991**, *221*, 37-47.
35 Hricovini, M.; Tvaroska, I.; Hirsch, J.; Duben, A. J. *Carbohydr. Res.* **1991**, *210*, 13-20.
36. Miller, K. E.; Mukhopadhyay, C.; Cagas, P.; Bush, C. A. *Biochemistry*, **1992**, *31*, 6703-6709, and references therein.
37. Discover 2.9 Program. Biosym Technol. Inc. San Diego, USA
38. Insight II 2.1.0. Program. Biosym Technol. Inc. San Diego, USA
39. (a) Forster, M.; Jones, C.; Mulloy, B. *J. Mol. Graph*, **1989**, *7*, 196-200. (b) Forster, M. J. *J. Comput. Chem.* **1991**, *12*, 292-302. *QCPE* program 636, Chemistry Department, Indiana Univ.,Bloomington, IN, 1992.

(*Received in UK* 9 *February* 1994; *revised* 21 *March* 1994; *accepted* 25 *March* 1994)